Gain, Phase, and Frequency Stability of DSS-42 and DSS-43 for Voyager Uranus Encounter

A. G. Cha
Radio Frequency and Microwave Subsystems Section

R. Levy
Ground Antennas and Facilities Engineering Section

In the present article, we derive theoretically rigorous definitions of such parameters as RF signal path length, phase delay, and phase/frequency stability in a Cassegrainian antenna applicable to a narrow bandwidth channel, as well as algorithms for evaluating these parameters. This work was performed in support of the Voyager spacecraft encounter with Uranus in January 1986. The information was needed to provide Voyager/Uranus radio science researchers with a rational basis for deciding the best strategy to operate the three antennas involved during the crucial 5-hour occultation period of the encounter. Such recommendations are made at the end of the article.

I. Introduction

The vast majority of Cassegrainian antenna articles are written about communications applications. The articles address well-defined communications characteristics of the antenna such as gain, sidelobe level, cross-polarization level, system gain over noise temperature ratio (G/T), and carrier over interference (C/I) ratio. The list above can be characterized as pertaining to the amplitude of the complex radiation pattern of the antenna. In recent years, the phase characteristics of the antenna radiation pattern have become extremely important for much scientific research in radio astronomy, geology, and planetary sciences. These phase characteristics include group delay time, phase delay, and Doppler shift (due to internal motion of antenna parts) in the antenna.

For large Cassegrainian antennas used in deep space communications and scientific research, normal operational practices based on communications considerations alone are often not sensible for scientific research where phase information is vital. In such applications, a careful balance must be maintained between the often conflicting communications requirements (gain) and antenna phase/frequency stability requirements dictated by scientific applications. An excellent example can be found in the NASA/JPL Deep Space

Network, where ground station antennas support both communications and scientific data acquisitions from outer space. For communications data acquisition, the subreflector is normally refocused to correct for gain loss due to gravity induced surface distortions, and the antenna is periodically con-scanned to peak up the gain. For VLBI and radio science applications, these gain-maximizing maneuvers are often deactivated to maintain better phase/frequency stability, but at the expense of sustaining some gain losses.

Given the importance of antenna phase characteristics in numerous scientific research projects, it is surprising that only scant information on phase-related characteristics can be found in parabolic and Cassegrainian reflector antenna literature. The paper by Cha, Rusch, and Otoshi appears to be the first rigorous analysis of RF signal group delay time through a reflector antenna (Ref. 1). In that paper, a GTD subreflector diffraction analysis and a physical optics main reflector diffraction analysis were made on a Cassegrainian antenna to determine the signal group delay on a theoretically rigorous basis. In the present article, we further derive theoretically rigorous definitions of such parameters as RF signal path length, phase delay, and phase/frequency stability in a Cassegrainian antenna applicable to a narrow bandwidth channel, as well as algorithms for evaluating these parameters. This work was performed in support of the Voyager spacecraft encounter with Uranus in January 1986. The information was needed to provide Voyager/Uranus radio science researchers with a rational basis for deciding the best strategy to operate the three antennas involved during the crucial 5-hour occultation period of the encounter. Such recommendations are made at the end of the article.

II. Mathematical Formulation of RF Signal Path Length, Phase Delay, and Doppler Shift in a Cassegrainian Antenna

The basis used to derive RF signal path length in a Cassegraininian antenna is ray optics and scalar diffraction theory. More elaborate diffraction theory can be used, but it has been shown that the simple approach described below yields an excellent approximation to a full two-reflector vector diffraction analysis insofar as delay characteristics in a large Cassegrainian antenna are concerned (Ref. 1). In Ref. 1, a rigorous two-reflector vector diffraction analysis was performed to determine RF signal group delay in a Cassegrainian antenna. The results were compared to results of a simpler analysis based on ray optics and aperture theory and were found to be nearly the same.

The procedure used to derive mathematical formulae for phase delay and Doppler shift is as follows. The well-known Kirchhoff scalar diffraction equation (variously known as Huygen's principle or aperture field integration method), is used to express the far field of a planar source of electromagnetic (EM) radiation. The amplitude and phase of the planar source are in turn determined from the feed horn radiation pattern using ray optics. The aperture field integration problem geometry is shown in Fig. 1. The source of radiation is the tangential components of the EM field (from Ref. 2, p. 161).

$$\bar{E}(R,\theta,\phi) = \frac{-jk}{4\pi R} \exp\left[-jk\,(R - R_o)\right] \hat{R} \times \int \{\hat{n} \times \bar{E}(\bar{R}') - \eta_o\, \hat{R} \times [\hat{n} \times \bar{H}(\bar{R}')]\} \cdot \exp\left(jk\bar{R}' \cdot \hat{R}\right) dS' \quad (1)$$

where

η_o = free space impedance

k = free space wave number

$\hat{R}$ = unit radial vector

$\hat{n}$ = unit normal vector to the aperture

In Eq. (1), the primed coordinate variables are the source coordinates and the unprimed coordinates are the field (observer) coordinates, all with an origin at point 0. The origin is selected away from the aperture center because a stationary origin relative to the ground is required. The aperture center, on the other hand, is a point that moves with the antenna pointing motion. Without loss of generality, assuming the E field is $\hat{y}$ polarized, the observer is in a direction normal to the aperture plane and ray optics is valid,

$$\hat{R} = \hat{n} = \hat{z} \quad (2)$$

$$\bar{E}(\bar{R}') = E_y(\bar{R}')\,\hat{y} \quad (3)$$

$$\bar{H}(\bar{R}') = -\frac{E_y(\bar{R}')}{Z_o}\,\hat{x} \quad (4)$$

Using Eqs. (2), (3), (4), Eq. (1) becomes

$$\bar{E}(R,0,0) = \frac{jk}{2\pi R} \exp\left[-jk\,(R - R_o)\right] \int E_y(\bar{R}')\, dS'\, \hat{y} \quad (5)$$

Dropping the vector notation in Eq. (5), and including the exp (jwt) time dependence hitherto suppressed,

$$E(R) = \frac{jk}{2\pi R} \exp\left[jwt - jk(R - R_o)\right] \int E_y(\bar{R}')\, dS' \quad (6)$$

Eq. (6) is used to precisely define such quantities as RF signal path length, phase delay, and Doppler shift in a Cassegrainian antenna in a manner that allows these quantities to be separated from other path length, phase delay, and Doppler in the overall signal propagation path.

With reference to Fig. 2, the path length is defined in the ray optics sense to start at the feedhorn phase center and end in the aperture plane. In Fig. 2, a typical ray pathlength is shown as $L_1 + L_2 + L_3$. The aperture plane is defined as the plane at a constant distance R_O from a stationary rotational axis (hour-angle axis for HA-dec antennas, azimuth axis for az-el antennas) in which the EM field has zero phase gradient (i.e., only quadratic phase error is present). Note that the paraboloid main reflector focal plane cannot generally be used as the aperture plane in our present formulation when the feedhorn or subreflector is not in a focused position. Our path length definition requires a number of rays to be used, an aperture plane to be found by searching (for a zero phase gradient plane), and ray path lengths to be averaged. The antenna beam peak, and not the main reflector axis, is assumed to be pointing at the spacecraft. This definition of antenna signal path length makes sense in that it neatly separates the antenna path length from other path lengths and phase delays in the signal propagation path, as will be shown.

Using ray optics, Eq. (6) can be written as

$$E(R) = \frac{\exp(jwt - jkR + jkR_0)}{R} \times \int |E(r', \phi')| \exp[-jk(L_1 + L_2 + L_3)]\, dS' \quad (7)$$

Equation (7) shows explicitly that the aperture field is derivable from ray optics and the phase of the aperture field is determined by the path lengths of rays originating from the feedhorn phase center. The constant factor $jk/2\pi$ has been omitted in Eq. (7) because it has no bearing on discussions in this article. We now define

$$L_s = L_1 + L_2 + L_3 = \text{total pathlength of individual ray} \quad (8)$$

$$E_o \exp(-jk\bar{L}_s) = \int E(r', \phi') \exp[-jk(L_1 + L_2 + L_3)]\, dS' = \text{illumination weighted average phase delay} \quad (9)$$

where E_o and $\bar{L}_s$ are real, positive numbers.

The quantity $\bar{L}_s$ in Eq. (9) is the average ray path length in the Cassegrainian antenna and is synonymous to RF signal path length in the antenna in this article. The phase and Doppler shift are then

$$\Delta\Phi = \text{phase change in antenna} = k\Delta\bar{L}_s \quad (10)$$

$$\Delta f = \text{Doppler shift due to } \frac{d\bar{L}_s}{dt} = (-)f\,\frac{\frac{d\bar{L}_s}{dt}}{c} \quad (11)$$

where

f = frequency

c = light velocity

The definition in Eq. (11) is justified as follows. Substituting Eq. (9) in Eq. (7),

$$E(R) = \frac{E_o}{R} \exp[j(wt - kR + kR_0 - k\bar{L}_s)] = \frac{E_o}{R} \cdot \exp(j\Phi) \quad (12)$$

where

$\Phi = \Phi(t)$ = phase as function of time

The instantaneous angular frequency is

$$\frac{d\Phi}{dt} = w - k\frac{dR}{dt} - k\frac{d\bar{L}_s}{dt} = w - kc\,\frac{\frac{dR}{dt}}{c} - kc\,\frac{\frac{d\bar{L}_s}{dt}}{c} = w - w\,\frac{\frac{dR}{dt}}{c} - w\,\frac{\frac{d\bar{L}_s}{dt}}{c} \quad (13)$$

where $w\,([dR/dt]/c)$ is the Doppler due to spacecraft motion and $w\,([d\bar{L}_s/dt]/c)$ is the Doppler due to internal motion in the antenna. To summarize:

$$\text{Phase change in antenna} = k\,\Delta\bar{L}_s \tag{14}$$

$$\text{Doppler shift} = (-)f\,\frac{\dfrac{d\bar{L}_s}{dt}}{c} \tag{15}$$

where $\Delta\bar{L}_s$ is the averaged path length change in the Cassegrainian antenna due to subreflector movement or surface deformation under varying gravity load conditions.

III. Phase Delay Change and Doppler Shift Due to Subreflector Motion Along z Axis

It is possible and useful to derive signal phase and frequency change caused by subreflector motion in terms of axial movement Δz and velocity $V_z = dz/dt$. As shown in Fig. 2, it is clear that a subreflector motion of Δz causes the overall pathlength to change by $2\Delta z$ approximately (Δz each in L_1 and L_2). Thus,

$$\Delta L_s \cong 2\Delta z \tag{16}$$

The factor of 2 is exactly correct for the ray (speaking in ray optics terms) on axis. When all ray path lengths are averaged, the theoretical computation by R. Levy[1] and experimental measurement of group delay time by Otoshi and Young (Ref. 3) suggest that the average path length change is more accurately given by

$$\Delta\bar{L}_s = 1.8\,\Delta z \tag{17}$$

It then follows that the phase delay change is

$$\Delta\text{PHASE} = 1.8k\,\Delta z \tag{18}$$

At first look, it would appear reasonable to use the axial (z-axis) velocity of the subreflector to arrive at a first-order estimate of the signal Doppler shift in antenna, $f(V_z/c)$. Comparing with Eq. (15), it becomes apparent that a better estimate may be $1.8f(V_z/c)$. The factor of 1.8 comes in from the folded optical path length $L_1 + L_2 + L_3$, as explained above. Substituting $\Delta\bar{L}_s = 1.8\,\Delta z$ in Eq. (15), we obtain the Doppler shift as $1.8f(V_z/c)$. To summarize in terms of z displacement and speed of subreflector (for $V_z/c \ll 1$):

$$\text{Phase delay change} = 1.8k\,\Delta z \tag{18}$$

$$\text{Doppler shift} = (-)1.8f(V_z/c) \tag{19}$$

[1]R. Levy, "X-Band Uplink D-Level Review on Antenna Mechanical Subsystem" (internal document), oral presentation at the Jet Propulsion Laboratory, Pasadena, Calif., July 1985.

It is hoped that someone who is familiar with the special theory of relativity can verify these. The relative merits of formulae for Eqs. (14) and (15) versus Eqs. (18) and (19) are as follows:

(1) Equations (14) and (15) are more accurate.

(2) Equations (18) and (19) are very simple to apply. The only relevant subreflector parameters are Δz and V_z. To use Eqs. (14) and (15), a detailed table of subreflector x, y, z position versus time is needed. The time dependence is non-trivially determined by computer programs in most large ground station antennas.

Insofar as Eqs. (18) and (19) are approximate formulae, some remarks and cautions are required. First, note that the z-axis subreflection motion is approximately parallel to the optical propagation path, while the x- and y-axis motions are approximately perpendicular to it. Therefore, the z-axis subreflector motion must be the dominant factor in phase change and Doppler determination. If one is faced with a situation where x- and y-axis displacements and velocities are an order or two of magnitude larger than z-axis motion, it is less clear when Eqs. (18) and (19) cease to be accurate approximations. The answer can probably come only from a large number of case studies. For the present, it is advised that Eqs. (14) and (15) be used when in doubt. In the meantime, Eqs. (18) and (19) do serve many useful purposes in providing quick estimates in cases where x- and y-axis motions are not orders of magnitude larger than z-axis motions.

IV. Numerical Results for Voyager Uranus Encounter

Three antennas are used in the Voyager closest encounter with Uranus, DSS-42 andDSS-43 in the NASA/JPL Deep Space Network, and the Australian Parkes antenna. During the 5-hour occultation period, the antennas are at (–)23° (337°) declination and sweep through the sky from approximately 335° (–25°) to 360° (0°), then to 50° in antenna (or local) hour-angle. The spacecraft location in antenna angular coordinates and the spacecraft occultation time from 0 to 5 hours in time are shown in Fig. 3. Note that every 15° in antenna hour-angle change corresponds to 1 hour in time. The chart in Fig. 3 is used to convert antenna angular coordinates from declination and hour angles to elevation and azimuth angles. As is well known, large ground-station antenna gain is dependent on the elevation angle because of gravity. During the 5-hour occultation period, the range of elevation angle is seen to be between 45° and 78°. The two antennas studied, DSS-42 and DSS-43, have diameters of 34 m and 64 m, respectively. The 34-m antenna has a HA-dec mount, while the 64-m antenna has an az-el mount. In the normal operation of the antennas, the subreflector is automatically refocused to

partially compensate for gain degradation induced by gravity as the elevation angle changes. This is especially important for the 34-m antenna, as the data will show. In addition, the entire antenna is periodically con-scanned to maintain pointing accuracy.

As stated previously, the radio science project scientists are highly concerned that the instruments used should not introduce either significant amplitude or phase distortions to signals returned from the spacecraft. It is desired that the antenna gain should be high as well as stay fairly constant over the range of elevation angles. For phase/frequency stability, it is believed that even a few degrees of phase change and/or a 0.01-Hz frequency shift introduced by the instrument could lead to loss of valuable scientific information (instrument sensitivity is such that a few degrees of phase change can be detected). Based on these considerations, the preliminary plan for tracking the spacecraft during occultation is as follows:

(1) The antennas will not be con-scanned but will be "blind-pointed" using pointing tables built into the control computer.

(2) The DSS-43 subreflector will be fixed instead of auto-focused.

(3) The DSS-42 subreflector will be auto-focused.

The reason for the different focusing techniques of DSS-42 and DSS-43 is that it is suspected that DSS-42 would sustain severe gain loss if it were not auto-focused.

The study reported herein was initiated in October 1985 to substantiate decisions (2) and (3) above and to determine the best position for fixing the DSS-43 subreflector. The results of our investigation are summarized in Tables 1 through 4 and cover the following cases:

Case I: DSS-43, subreflector fixed at position for 42° elevation.

Case II: DSS-43, subreflector fixed at position for 67° elevation.

Case III: DSS-42, subreflector auto-focused.

Case IV: DSS-42, subreflector fixed at position for 67° elevation.

The independent variable for the tables is mission time, tabulated in the first column. The tables are intended to show how the antenna gain, phase, and Doppler shift vary within the 5-hour occultation period. The gain variation is computed from a theoretical structural deformation model, including the RMS surface error loss and defocusing loss in cases where the subreflector is not auto-focused. For Cases I, II, and IV, the phase and frequency changes are computed from Eqs. (14) and (15), again using the theoretical structural deformation model. For these cases, the subreflector is fixed, and the antenna phase/frequency instability is caused by the continuous smooth (small-scale) reflector surface deformation under varying gravity load conditions, resulting in excellent antenna phase/frequency stability. For Case III, the antenna phase/frequency changes are computed from Eqs. (18) and (19). In this case, the subreflector is auto-focused and the phase/frequency stability is determined largely by subreflector motion rather than the main reflector structural deformation. Although it is preferable to use the exact Eqs. (14) and (15), it is difficult to determine a detailed subreflector position versus time table (i.e., x, y, z versus T), due to the complexity of the subreflector-motion controlling computer program. Since a quick but only approximate answer was needed, Eqs. (18) and (19) were chosen for use in this case. For DSS-43 (64-m antenna), it is clear from Tables 1 and 2 that the subreflector should be fixed at the position corresponding to a 67° elevation angle, by virtue of higher absolute gain and much smaller gain variation over the range of elevation angles of concern. For DSS-42 (34-m antenna), a comparison of Tables 3 and 4 substantiates the decision to auto-focus the subreflector, in view of the large gain loss and gain variation seen in Case IV. The phase/frequency stability of Case III is much worse, as expected, due to subreflector focusing movement. The Doppler shift reflects the way the subreflector is designed and/or programmed to move – the focusing motion comes in short spurts of constant-velocity motion of 0.0023 in./sec along the z axis and lasts about 10 seconds or so. This leads to a ±0.0029-Hz phase stability prediction at X-band based on Eq. (19).

The following background information should be a helpful supplement to the tables:

(1) The case with DSS-43 subreflector auto-focused was not included. For this case, X-band Δf = 0.03 Hz; X-band Δphase = 22° over a 2-second period sporadically. The phase and frequency changes are computed from Eqs. (18) and (19). In this case, the subreflector is programmed to move only when the position error (relative to focused position for maximum gain) in either x, y, or z axis is at least 0.0488 in. The subreflector z-axis velocity is 0.024 in./sec, leading to the rather significant 0.03-Hz Doppler shift.

(2) All X-band Δphase and Δf numbers can be multiplied by (f_s/f_x) to obtain S-band numbers.

(3) The tables are for ΔT = 20 min. For cases where the subreflector is auto-focused, it is predicted that the frequency and phase changes take place sporadically in short periods of a few seconds in the 20-minute timespan. If needed, it appears possible that a subreflector position versus time history, i.e., (x, y, z) versus T for ΔT = a few seconds, may be obtained through a combination of operator console actions and the use of chart recorders at each antenna.

(4) The possibility of focusing the subreflector in x-and y-axes and fixing the subreflector z-axis position during occultation has been suggested. This appears a viable alternative, especially for DSS-42. Using this option, the gain loss with elevation-angle characteristics is believed to be only a couple of hundredths of a dB worse than full three-axis focusing, while the frequency stability is believed to be a couple of orders of magnitude better than the full three-axis focusing case.

V. Conclusions and Recommendations

For the Voyager Uranus encounter, the original plan (in late October 85) was to fix the DSS-43 subreflector at position of 42° elevation angle while auto-focusing the DSS-42 subreflector during occultation. The rationale has been explained above. The investigation described herein has substantiated the soundness of the different approaches to operating the two antennas. In addition, the optimal elevation angle for the DSS-43 subreflector has been determined. The results of the investigation support the following approach:

(1) A fixed DSS-43 subreflector position of 67° elevation angle.

(2) Auto-focusing the DSS-42 subreflector in x- and y-axes only.

In addition, rigorous formulations and exact definitions have been presented of parameters such as path length, phase delay, and Doppler shift in the antenna that do not appear to exist in a consistent and exact manner.

References

1. Cha, A. G., Rusch, W. V. T., and Otoshi, T., "Microwave Delay Characteristics of Cassegrainian Antennas," *IEEE Trans. on Antennas and Propagation*, Vol. AP-26, No. 6, pp. 860–865, Nov. 1978.

2. Silver, S., editor, *Microwave Antenna Theory and Design*, McGraw Hill, 1949.

3. Otoshi, T., and Young, L., "An Experimental Investigation of the Changes of VLBI Time Delays Due to Antenna Structural Deformations," *TDA Progress Report 42-68*, pp. 8–16, Jet Propulsion Laboratory, Pasadena, Calif., April 15, 1982.

Table 1. DSS-43 (64 m) X-band subreflector fixed at position for 42° elevation, declination = 337° (-23°)

Mission Times, hr-min	Antenna Hour Angle, deg	Antenna Elevation Angle, deg	Subreflector Position, in.			Relative Gain, dB[1,2]	ΔPhase, deg	Cumulative ΔPhase, deg	ΔFreq, μHz (Hz X 10^{-6})
			x	*y*	*z*				
0 – 0	335	65		↑		−0.35	0.0	0.0	--
0 – 20	340	69				−0.47	0.3	0.3	−0.85
0 – 40	345	72				−0.60	0.5	0.8	−0.78
1 – 0	350	75				−0.72	0.3	1.1	−0.64
1 – 20	355	77				−0.81	0.3	1.4	−0.35
1 – 40	0	78	No *x* motion in normal antenna operation, *y*, *z*			−0.85	0.0	1.4	0.0
2 – 0	5	77	normally refocused, fixed			−0.81	−0.3	1.1	+0.35
2 – 20	10	75	for occultation:			−0.72	−0.3	0.8	+0.64
2 – 40	15	72				−0.60	−0.5	0.3	+0.78
3 – 0	20	69		*y* = +0.18		−0.47	−0.3	0.0	+0.85
3 – 20	25	65		*z* = −0.04		−0.35	−0.5	−0.5	+0.85
3 – 40	30	61				−0.24	−0.3	−0.8	+0.78
4 – 0	35	57				−0.15	−0.3	−1.1	+0.74
4 – 20	40	53				−0.08	−0.3	−1.4	+0.67
4 – 40	45	49				−0.03	−0.3	−1.7	+0.59
5 – 0	50	45				0.0	--	--	--
5 – 20	55	41		↓		--	--	--	--

Notes:

1. Gain reference: 0 dB is at rigging angle of 45° elevation; subreflector is focused.
2. Relative gain loss includes surface deformation and defocusing effects due to gravity. However, pointing loss is not included.

Table 2. DSS-43 (64 m) X-band subreflector fixed at position for 67° elevation, declination = 337° (-23°)

Mission Times, hr-min	Antenna Hour Angle, deg	Antenna Elevation Angle, deg	Subreflector Position, in.			Relative Gain, dB[1,2]	ΔPhase, deg	Cumulative ΔPhase, deg	ΔFreq, μHz (Hz × 10^{-6})
			x	y	z				
0 – 0	335	65		↑		−0.04	0.0	0.0	--
0 – 20	340	69				−0.06	0.3	0.3	−0.85
0 – 40	345	72				−0.10	0.5	0.8	−0.78
1 – 0	350	75				−0.13	0.3	1.1	−0.64
1 – 20	355	77				−0.17	0.3	1.4	−0.35
1 – 40	0	78	No x motion in normal antenna operation. y, z			−0.18	0.0	1.4	0.0
2 – 0	5	77	normally refocused, fixed			−0.17	−0.3	1.1	+0.35
2 – 20	10	75	for occultation:			−0.13	−0.3	0.8	+0.64
2 – 40	15	72				−0.10	−0.5	0.3	+0.78
3 – 0	20	69		$y = -1.53$		−0.06	−0.3	0.0	+0.85
3 – 20	25	65		$z = +0.25$		−0.04	−0.5	−0.5	+0.85
3 – 40	30	61				−0.05	−0.3	−0.8	+0.78
4 – 0	35	57				−0.08	−0.3	−1.1	+0.74
4 – 20	40	53				−0.12	−0.3	−1.4	+0.67
4 – 40	45	49				−0.19	−0.3	−1.7	+0.59
5 – 0	50	45				--	--	--	--
5 – 20	55	41		↓		--	--	--	--

Notes:

1. Gain reference: 0 dB is at rigging angle of 45° elevation; subreflector is focused.
2. Relative gain loss includes surface deformation and defocusing effects due to gravity. However, pointing loss is not included.

Table 3. DSS-42 (34 m) X-band subreflector auto-focused, declination = 337° (-23°)

Mission Times, hr-min	Antenna Hour Angle, deg	Subreflector Position, in.			ΔGain, dB	ΔPhase deg	Cumulative ΔPhase deg	ΔFreq. μ Hz (Hz X 10^{-6})
		x	y	z				
0 – 0	335	1.013	0.894	0.055	−0.17	0.0	0.0	
0 – 20	340	0.820	0.912	0.060	−0.17	2.3	2.3	
0 – 40	345	0.621	0.927	0.064	−0.16	1.8	4.1	
1 – 0	350	0.416	0.437	0.067	−0.16	1.4	5.5	
1 – 20	355	0.209	0.944	0.068	−0.16	0.5	6.0	
1 – 40	0	0.000	0.946	0.069	−0.16	0.5	6.5	
2 – 0	5	−0.209	0.944	0.068	−0.16	−0.5	6.0	
2 – 20	10	−0.416	0.937	0.067	−0.16	−0.5	5.5	±2900 Hz over duration of a few seconds
2 – 40	15	−0.621	0.927	0.064	−0.16	−1.4	4.1	
3 – 0	20	−0.820	0.912	0.060	−0.17	−1.8	2.3	
3 – 20	25	−1.013	0.896	0.055	−0.17	−2.3	0.0	
3 – 40	30	−1.199	0.872	0.049	−0.17	−2.8	−2.8	
4 – 0	35	−1.375	0.846	0.042	−0.18	−3.2	−6.0	
4 – 20	40	−1.541	0.816	0.034	−0.18	−3.7	−9.7	
4 – 40	45	−1.695	0.784	0.025	−0.19	−4.1	−13.8	
5 – 0	50	−1.837	0.748	0.016	--	−4.1	−17.9	
5 – 20	55	−1.964	0.710	0.006	--	−4.6	−22.5	
5 – 40	60	−2.077	0.670	−0.005	--	−4.6	−27.1	

Notes:

1. Gain reference: 0.dB is at rigging angle of 40° elevation; subreflector is focused.
2. Relative gain loss includes surface deformation and defocusing effects due to gravity. However, pointing loss is not included.
3. Receding subreflector (going away from feed/main reflector) leads to positive Δphase and negative Δfrequency.

Table 4. DSS-42 (34 m) X-band subreflector fixed at 67° elevation, declination = 337° (-23°)

Mission Times, hr-min	Antenna Hour Angle, deg	Subreflector Position, in.			ΔGain, dB	ΔPhase, deg	Cumulative Δ Phase, deg	ΔFreq. μ Hz (Hz X 10^{-6})
		x	y	z				
0 – 0	335		↑		−0.45	0.0	0.0	−1.9
0 – 20	340				−0.36	0.8	0.8	−1.6
0 – 40	345				−0.27	0.5	1.3	−1.2
1 – 0	350				−0.21	0.5	1.8	−0.8
1 – 20	355				−0.17	0.3	2.1	−0.4
1 – 40	0				−0.17	0.	2.1	0.0
			x = 0.82 in.					
2 – 0	5		y = 0.91 in.		−0.17	−0.3	1.8	+0.4
2 – 20	10		z = 0.06 in.		−0.21	−0.5	1.3	+0.8
2 – 40	15		for el = 67°		−0.27	−0.5	0.8	+1.2
3 – 0	20		(HA = 340°)		−0.36	−0.8	0.0	+1.6
3 – 20	25				−0.45	−1.0	−1.0	+1.9
3 – 40	30				−0.57	−1.0	−2.0	+2.3
4 – 0	35				−0.70	−1.3	−3.3	+2.7
4 – 20	40				−0.84	−1.3	−4.6	+3.3
4 – 40	45				−0.99	--	--	--
5 – 0	50				--	--	--	--
5 – 20	55				--	--	--	--
5 – 40	60		↓		--	--	--	--

Notes:

1. Gain reference: 0 dB is at rigging angle of 40° elevation; subreflector is focused.
2. Relative gain loss includes surface deformation and defocusing effects due to gravity. However, pointing loss is not included.

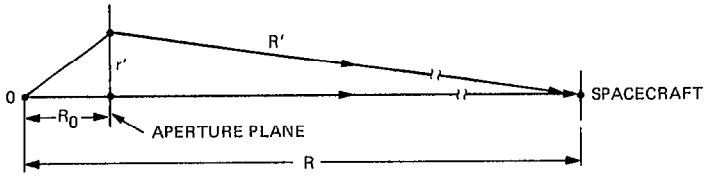

Fig. 1. Coordinate systems in aperture field integral

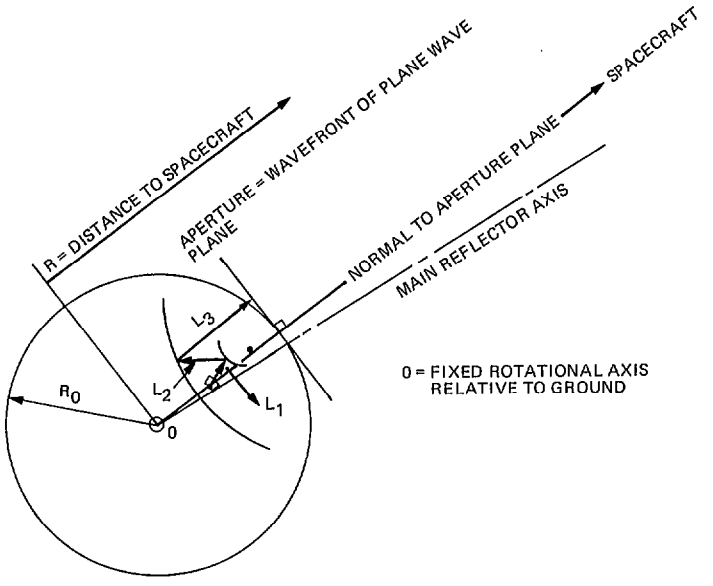

Fig. 2. Defining aperture plane and ray path length

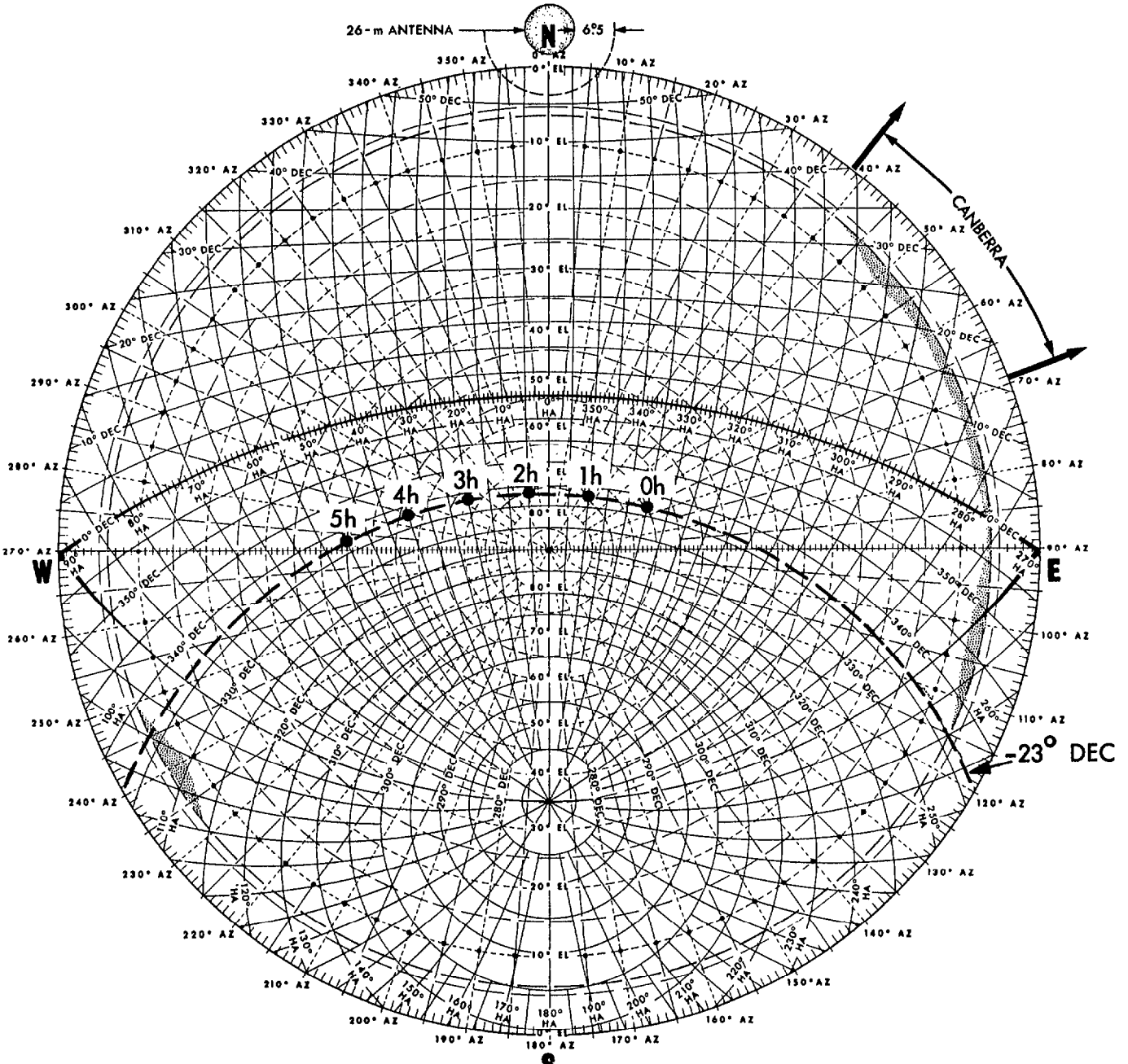

ELEVATION LIMITS		AZIMUTH LIMITS	
EL PRE	FINAL	AZ* PRE	FINAL
+6.0	5.4	CW TO 40	42.5
+89.0	89.3	CCW TO 230	227.5
* STARTING FROM 0° AZ, OR TRUE NORTH			

BALLIMA STATION, DSS 43

AZ-EL AND HA-DEC COORDINATES
STEREOGRAPHIC PROJECTION

FORM JPL 0974-2, 11/72

Fig. 3. DSS-42 and -43 Az-El and HA-Dec coordinates for Voyager Uranus Encounter